

Oxidation degree dependent adsorption of ssDNA onto graphene-based surface

Huishu Ma(马慧姝), Jige Chen(陈济舸), Haiping Fang(方海平), and Xiaoling Lei(雷晓玲)

Citation: Chin. Phys. B, 2021, 30 (**10**): 106806. DOI: 10.1088/1674-1056/abf109
Journal homepage: http://cpb.iphy.ac.cn; http://iopscience.iop.org/cpb

What follows is a list of articles you may be interested in

Tolman length of simple droplet: Theoretical study and molecular dynamics simulation

Shu-Wen Cui(崔树稳), Jiu-An Wei(魏久安), Qiang Li(李强), Wei-Wei Liu(刘伟伟), Ping Qian(钱萍), and Xiao Song Wang(王小松)

Chin. Phys. B, 2021, 30 (**1**): 016801. DOI: 10.1088/1674-1056/abb65a

Influence of external load on friction coefficient of Fe-polytetrafluoroethylene

Xiu-Hong Hao(郝秀红), Deng Pan(潘登), Ze-Yang Zhang(张泽洋), Shu-Qiang Wang(王树强), Yu-Jin Gao(高玉金), Da-Peng Gu(谷大鹏)

Chin. Phys. B, 2020, 29 (**4**): 046802. DOI: 10.1088/1674-1056/ab7da0

Approximate expression of Young's equation and molecular dynamics simulation for its applicability

Shu-Wen Cui(崔树稳), Jiu-An Wei(魏久安), Wei-Wei Liu(刘伟伟), Ru-Zeng Zhu(朱如曾), Qian Ping(钱萍)

Chin. Phys. B, 2019, 28 (**1**): 016801. DOI: 10.1088/1674-1056/28/1/016801

Effect of isotope doping on phonon thermal conductivity of silicene nanoribbons: A molecular dynamics study

Run-Feng Xu(徐润峰), Kui Han(韩奎), Hai-Peng Li(李海鹏)

Chin. Phys. B, 2018, 27 (**2**): 026801. DOI: 10.1088/1674-1056/27/2/026801

Effect of amorphous lamella on the crack propagation behavior of crystalline Mg/amorphous Mg-Al nanocomposites

Hai-Yang Song(宋海洋) and Yu-Long Li(李玉龙)

Chin. Phys. B, 2016, 25 (**2**): 026802. DOI: 10.1088/1674-1056/25/2/026802

Oxidation degree dependent adsorption of ssDNA onto graphene-based surface*

Huishu Ma(马慧姝)[1,2], Jige Chen(陈济舸)[1,4], Haiping Fang(方海平)[3,4], and Xiaoling Lei(雷晓玲)[3,†]

[1] *Division of Interfacial Water and Key Laboratory of Interfacial Physics and Technology, Shanghai Institute of Applied Physics, Chinese Academy of Sciences, Shanghai* 201800, *China*
[2] *University of Chinese Academy of Sciences, Beijing* 100049, *China*
[3] *Department of Physics, East China University of Science and Technology, Shanghai* 200237, *China*
[4] *Shanghai Synchrotron Radiation Facility, Zhangjiang Laboratory, Shanghai Advanced Research Institute, Chinese Academy of Sciences, Shanghai* 201210, *China*

(Received 7 January 2021; revised manuscript received 4 March 2021; accepted manuscript online 23 March 2021)

DNA/GO composite plays a significant role in the research field of biotechnology and nanotechnology, and attracts a great deal of interest. However, it is still unclear how the oxidation degree of the graphene-based surface affects the adsorption process of single-strand DNA (ssDNA). In this paper, based on the molecular dynamics simulations, we find that ssDNA molecule is absorbed on the GO surface in the most stable state with the oxidation degree around 15%. The microscopic mechanism is attributed to the van Der Walls and the electrostatic interactions between the ssDNA molecule and the graphene-based surface, which is accompanied with the π–π stacking and hydrogen bond formation. The number of π–π stacking between ssDNA and GO reaches the maximum value when the oxidation degree is around 15% among all the GO surfaces. Our simulation results also reveal the coexistence of stretched and curved configurations as well as the adsorption orientation of ssDNA on the GO surface. Furthermore, it is found that the absorbed ssDNA molecules are more likely to move on the graphene-based surface of low oxidation degree, especially on pristine graphene. Our work provides the physics picture of ssDNA's physisorption dynamics onto graphene-based surface and it is helpful in designing DNA/GO nanomaterials.

Keywords: single-strand DNA (ssDNA), molecular dynamics simulation, oxidation degrees, graphene-based surfaces

PACS: 68.43.Mn, 68.47.Gh, 87.14.gk, 34.35.+a **DOI:** 10.1088/1674-1056/abf109

1. Introduction

DNA, the carrier of genetic information, participates in most of the bio-functional processes such as the replication, transcription and plays a pivotal role in living organisms.[1,2] Recently, with the rapid advance in biotechnology and nanotechnology, DNA-functionalized nanomaterials, such as DNA/GO,[3] DNA/Au,[4] and DNA/MFe_2O_4,[5] exhibit extensively development as new applications of DNA in biosensors,[3,6,7] biomedicine,[8,9] nanotechnology,[10] and materials science.[11–13] Among these applications, the combination of DNA and graphene, the first two-dimensional (2D) atomic crystal available to us, attracts a great deal of interest. Graphene exhibits many extraordinary properties, such as high surface area,[14] fast electron mobility,[15] good optical transparency,[16,17] high Young's modulus,[18] and excellent thermal conductivity,[19] which can be exploited for numerous applications in energy, environment,[20] and biomedicine.[21] To enhance its dispersion in aqueous solution for numerous applications, graphene is usually oxidized to be graphene oxide (GO), which mainly bears carboxylic groups on its edges, hydroxyl and epoxy groups on its basal plane. These oxidative functional groups increase the biocompatibility of GO through the formation of both covalent and non-covalent bonds with biomolecules.[22]

Recently, the combination of DNA and GO has inspired a lot of innovative work,[23,24] and practical applications,[25,26] especially in the biosensors. The application of DNA/GO nanomaterials is based on that single-stranded DNA (ssDNA) has a preferential binding on GO compared to double-stranded DNA (dsDNA), because of non-covalent interactions with the surface.[27–30] The main interactions between ssDNA molecules and GO have been recognized as hydrophobic,[31,32] hydrogen bonding,[21,33] and π–π stacking interactions[29,33] by both theoretical and experimental methods. The dynamic interactions between DNA molecule and GO surface are complex and depend on the sequences and length of DNA[34,35] as well as the surface defects and surface properties of GO.[36]

As we known, the oxidized groups are not evenly distributed on the GO surface.[37,38] Within the GO plane, there

*Project supported by the National Natural Science Foundation of China (Grant Nos. 11305237 and 11974366), the Fundamental Research Funds for the Central Universities, China, the Natural Science Foundation of Shanghai, China (Grant No. 19ZR1463200), and the Key Research Program of Chinese Academy of Sciences (Grant No. QYZDJ-SSW-SLH053).

†Corresponding author. E-mail: leixiaoling@ecust.edu.cn

© 2021 Chinese Physical Society and IOP Publishing Ltd

is the coexistence of both large unoxidized and oxidized regions proved by experimental and theoretical works. Even in oxidized regions, there are some small areas of sp^2-hybridized domains, similar to "islands",[39–43] because of the steric effects. This uneven oxidized groups distribution on GO makes its surface polarity complex. Generally, surface polarity is known as an important factor for the dynamic adsorption process and the configurations of biomolecules.[44–46] Yan *et al.* investigated the effects of the oxidation degree (OD) on MB adsorption behavior systematically, indicating that the dye uptakes of GO exponentially increase with the increase of OD.[46] The relationship among the degree of oxidation, defects of GO and the adsorption performance was investigated by Tan *et al.* The results showed that the adsorption of Cu^{2+} on GO was strongly dependent on the oxidation degree and independent of the defects under various pH levels and ionic strength.[47] Tu *et al.* found that the complex surface polarity of GO was crucial to the antibacterial activity of the material based on the experiments and the molecular dynamic simulation.[48] For DNA-surface interactions, experimental study demonstrated that the formation of interfacial hydrogen bonds between DNA and GO was crucial for the attachment of ssDNA and the detachment of hybridized dsDNA during the sensing process.[27] It was obvious that the density of polar groups on the graphene surface or oxidation rate have a direct implication on physisorption process and these interactions can either enhance or reduce the biocompatibility and stability of ssDNA on graphene-based surfaces. Most of the previous studies about the DNA adsorption on GO did not consider the effect of oxidation degree of GO. Kim *et al.* performed a detailed investigation of the effect of surface oxidation rate of graphene surfaces on the physisorption process of $poly(T)_{20}$ based on all-atomic MD simulations. However, they only considered the GO sheets that the hydroxyl and epoxy groups were grafted on both sides of the surface in a random manner.[49]

Here, based on Shi–Tu model, we performed all-atom molecular dynamics (MD) simulations to investigate the physisorption of ssDNA onto graphene-based surfaces with oxidation degrees from 0 to 25%. From the results, we found ssDNA molecule was absorbed in most stable state on the GO surface with the oxidation degree around 15% due to the maximum value of interaction. By analyzing the distinguished interaction between graphene-based surfaces and ssDNA molecules, we found that the electrostatic interaction increased with the oxidation degree of graphene-based surface. And the Van Der Walls (vdW) interaction first increases and then decreased with the oxidation degree, holding the greatest value for the GO of 15% oxidation degree. The result was also confirmed by the number of π–π stacking between them. Further analysis showed that, the less oxidation degree on graphene-based surface, the greater probability for ssDNA to form the approximately parallel configuration, regardless of the coexistence of both stretched and curved configurations. Our work revealed the oxidation degree dependent absorption of ssDNA molecules onto graphene-based surface and provided theoretical guidance for the application of DNA/GO nanomaterials.

2. Methods

2.1. Structure of ssDNA and graphene-based surfaces

In this study, the ssDNA molecule with the base sequence 5'-ATGCATGCATGC-3', $(ATGC)_3$, was used. The initial $(ATGC)_3$structure was built using nucleic acid builder (NAB) in AMBER 14 package. The model of graphene-based materials was constructed based on the high correlation between oxidation loci, as reported by Yang *et al.*[50] Using this model, various oxidation degrees (from 0 to 25%, in 5% increments), $d_O = n_O/n_C$, where n_O and n_C were the number of oxygen atoms and carbon atoms, respectively, explored in this study were achieved. Representative snapshots of the surfaces were shown in Fig. S1.

The ssDNA molecule was placed on the graphene-based surface with the helix axis parallel to the basal plane of graphene-based which had dimensions of 10.084×10.224 nm^2. The centroid distance between the graphene-based surface and ssDNA molecule was 3 nm. To investigate the effects of oxidation degree on adsorption, eight samples of each oxidation degree were constructed. The whole system was filled with water molecules, and sodium ions were added to neutralize the negative charges of the ssDNA molecule.

2.2. MD simulation

The simulation box was $10.084 \times 7.00 \times 10.224$ nm^3 in x, y and z direction, and the periodic boundary was applied to all x, y and z three directions. All simulations were performed in the NVT ensemble at 300 K by GROMACS 4.5.4.[51] We chose the Amber03 force filed[52] to simulate the ssDNA molecule, which had been widely used in DNA simulations.[53–56] The detailed force field parameters of graphene-based surfaces were consistent with our previous publication.[34,35,57] As for the simulation model of graphene-based materials, the carbon atoms were presented as the uncharged Lennard–Jones particles with the vdW parameters of $\sigma_{CC} = 3.58$ Å and $\varepsilon_{CC} = 0.0663$ kcal·mol^{-1}.[58–60] The balance length of C–C bond was set to be 0.142 nm by the harmonic potentials with the spring constants of 322.55 kcal·mol^{-1}·Å^{-2}. The vibration of the C–C–C angle was also simulated by the harmonic

potentials with the balanced angle of 120° and spring constants of 53.35 kcal·mol^{-1}·rad^{-2}. And the planar dihedral angles between C–C–C–C was kept by the spring constants of 3.15 kcal·mol^{-1}. The simulation parameters of –OH, –O–, and –COOH groups on the graphene-based surface were set according to the Amber03 force filed. The TIP3P model was used.[61] The long-range electrostatic interaction was treated with the particle-mesh Ewald method[62] with a real space cutoff of 1.2 nm. The cutoff distance of the vdW interaction was set up to be 1.2 nm as well.

Initially, the system equilbration was performed in the NPT ensemble and was simulated for 5 ns, where the ssDNA molecule was constrained by position restraints. Then, the constraints were removed and the production simulations were run in the NVT ensemble for 400 ns. The time step in all simulations were set to be 2 fs and the data were collected every 2 ps.

3. Results and discussion

The control MD simulation systems were designed to investigate the ssDNA physisorption dynamics on the pristine graphene (PG) and GO with various oxidation degrees from 5% to 25% (GO-5%, GO-10%, GO-15%, GO-20%, and GO-25%). GO surfaces were constructed based on the Shi–Tu structure model, on which the distribution of oxidized groups was generated according to the rate-constant ratios from the computation by combining the density functional theory and conventional transition-state theory. As shown in Fig. S1(b), the GO nanosheets could be divided into low oxidation degree (PG and GO-5%), moderate oxidation degree (GO-10%, GO-15%) and high oxidation degree (GO-20%, GO-25%). For low oxidation degree GO nanosheets, the unoxidized region dominated the GO surface. For moderate oxidation degree GO nanosheets, both large unoxidized and oxidized regions coexisted on the surface. For high oxidation degree GO nanosheets, the oxidized region dominated the GO surface. However, even though the oxygen groups distributed over all the surface of GO-25%, small areas of sp^2-hybridized domains, similar to "islands", were formed over all the surface. In all systems, the ssDNA molecules were initially placed above the graphene-based surface with the helix axis parallel to the basal plane and the centroid distance of 3 nm in y axis (Fig. S1(a)).

3.1. Interaction between ssDNA and graphene-based surface

Figure 1(a) showed the typical snapshots of adsorbed ssDNA molecules on various oxidation degrees GO surfaces from 0 to 25% at 400 ns and all snapshots were shown in Fig. S2. It was clearly that ssDNA molecules could be adsorbed on graphene-based surface as various kinds of configurations. And even on the same graphene-based surface, the absorbed ssDNA molecules could display as stretched or curved configurations. We calculated the averaged total interaction energy between ssDNA and graphene-based surface, including electrostatic and vdW interactions, both of which dominated the adsorption process. As shown in Fig. 1(b), we found that the total interaction energy between ssDNA molecules and GO-15% held the value of −1161.87 kJ/mol, which was not only larger than that of other oxidation degree GO surfaces but also of PG. The result suggested that ssDNA molecule was absorbed in the most stable state on the GO surface with the oxidation degree around 15%, rather than PG or other GO surfaces.

In order to analyze the detailed interaction between adsorbed ssDNA and graphene-based surface, we analysed the changing of the electrostatic and vdW interactions individually with the oxidation degrees. From the result, it was noted that the electrostatic interaction increased with the oxidation degree of surface from 0 kJ/mol to −258.43 kJ/mol due to the increased number of oxidized groups on GO surfaces. For the vdW interaction energy, the PG held the maximum value of −999.99 kJ/mol, larger than that of any GO surfaces. Because of the steric effect formed by the oxidized groups on GO surface, the moving area was prevented when the aromatic rings of the nucleobases adjusted its configurations to forming π–π stacking structure with the GO surface. Interestingly, we found that the vdW interaction between ssDNA and GO surface did not increase or decrease monotonically with the oxidation degree of GO. GO-15% held the value of −992.15 kJ/mol, which was the greatest vdW interaction among all GO surfaces except the PG surface. Due to the energetic properties can be further decomposed into the contribution of the oxygen-containing and non-oxygen-containing groups on the surface, we also calculated the averaged total interaction energy between ssDNA and graphene-based surface, including oxygen-containing and non-oxygen-containing groups regions interactions. As shown in Fig. S7, for the non-oxygen-containing groups regions interaction energy, the PG held the maximum value of −960.82 kJ/mol, larger than that of any GO surfaces. Interestingly, we also found that the non-oxygen-containing groups regions interaction between ssDNA and GO surface did not increase or decrease monotonically with the oxidation degree of GO. GO-15% held the value of −686.61 kJ/mol, which was the greatest non-oxygen-containing groups regions interaction among all GO surfaces except the PG surface. And the oxygen-containing groups regions interaction increased with the oxidation degree of surface from 0 kJ/mol to −679.10 kJ/mol due to the increased number of oxidized groups on GO surfaces.

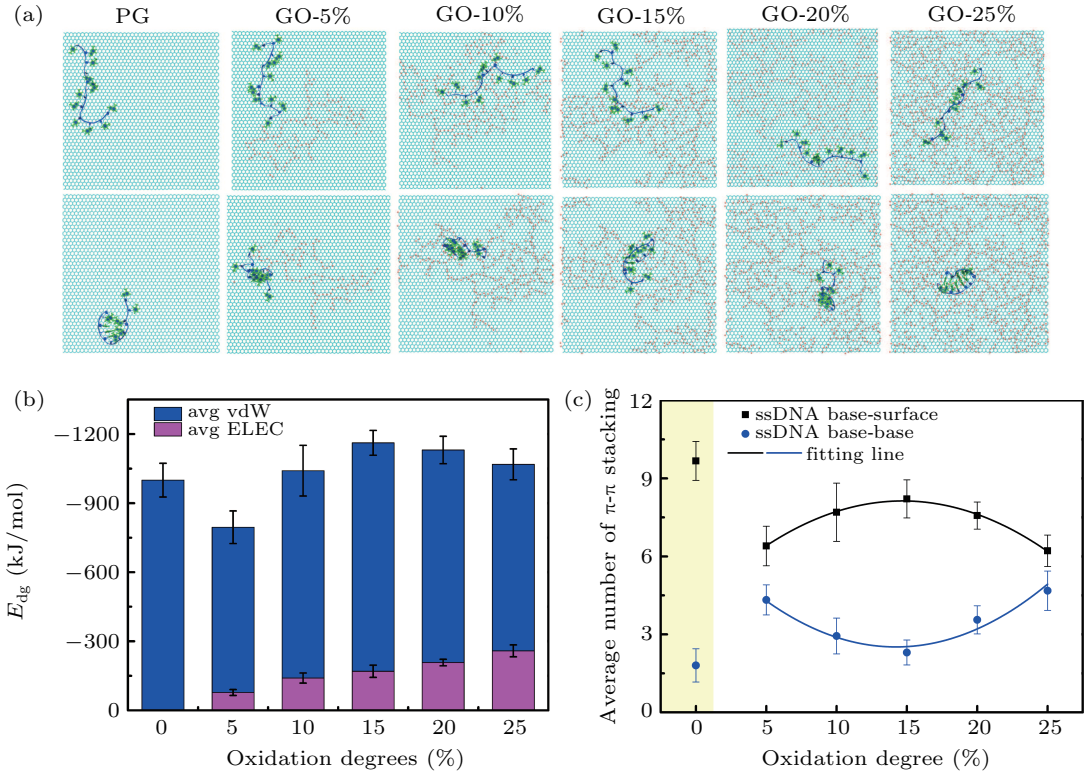


Fig. 1. (a) Typical simulation snapshots of stretched and curved structures of ssDNA adsorbed on the PG, GO surface around 5%, 10%, 15%, 20% and 25% oxidation degree. The oxygen and hydrogen atoms on GO were shown as red and white spheres, respectively. The carbon atoms were represented in the cyan line. The phosphate backbone and nucleobases of ssDNA were shown by the blue lines and green bonds, respectively. (b) Average interaction energy between ssDNA and graphene-based surface with variable oxidation degrees. The vdW and electrostatic contributions to non-bonded energy were colored as blue and magenta, respectively. (c) Average number of the intra π–π stacking structures of ssDNA molecules (base stacking, blue circles) and the inter π–π stacking structures between ssDNA molecules and graphene-based surface (base-surface stacking, black squares).

To clearly characterize the vdW interaction, we calculated the number of π–π stacking between ssDNA molecule and graphene-based surface, as shown in Fig. 1(c). We found that PG nanosheet processes the maximum number of π–π stacking with ssDNA molecule. It was noted that the relation between the number of π–π stacking and oxidation degree was not monotonous but similar to that between the vdW interaction and oxidation degree. Moreover, the quantitative functional relationship between them could be concluded as $y_1 = -0.018x^2 + 0.538x + 4.175$. Furthermore, the number of π–π stacking inside the ssDNA molecules held the opposite trend with that between ssDNA and GO of the relation function of $y_2 = 0.021x^2 - 0.592x + 6.729$. As for the PG, the number of π–π stacking with ssDNA molecules was greater than any GO surfaces, which was consistent with previous studies[63,64] and also the result of vdW interaction. From the changing trend of the electrostatic and vdW interaction, the GO-15% surface processed the most stable adsorption with the ssDNA molecules.

3.2. Dynamic processes of ssDNA adsorption on graphene-based surface

In order to figure out the underlying function mechanism of the oxidized groups on the dynamic adsorption process of ssDNA molecules on graphene-based surface, we calculated the interaction energy (E_{dg}) together with the number of π–π stacking and the hydrogen bond. The absorbed ssDNA had been distinguished as stretched or curved configurations. The results of PG and GO-5% were shown in Fig. 2 and the other results were shown in Figs. S4 and S5. From these figures, we noted that E_{dg} decreased with the simulation time, indicating the dynamic adsorption process of ssDNA molecule onto the graphene-based surface. The stepwise decrease in E_{dg} was accompanied with the forming of π–π stacking configurations between ssDNA molecules and graphene-based surface, suggesting that the absorbed configuration became more stable step by step. Electrostatic interaction mainly contributed to the physisorption process by forming of hydrogen bonds, which was greatly dependent on the oxidation degree of graphene-based surface. With the increasing of the oxidation degree, the electrostatic interaction between ssDNA and GO surface increased, which was companied with the increasing number of hydrogen bonds.

As for the PG, ssDNA molecule could be stably absorbed on its surface in less than 65 ns as stretched configuration and keep stable to 400 ns with some fluctuation. As curved configuration, the stable adsorption time was much longer of 156 ns. By comparing these two absorption configurations, we figured out that ssDNA molecule was more likely to be absorbed

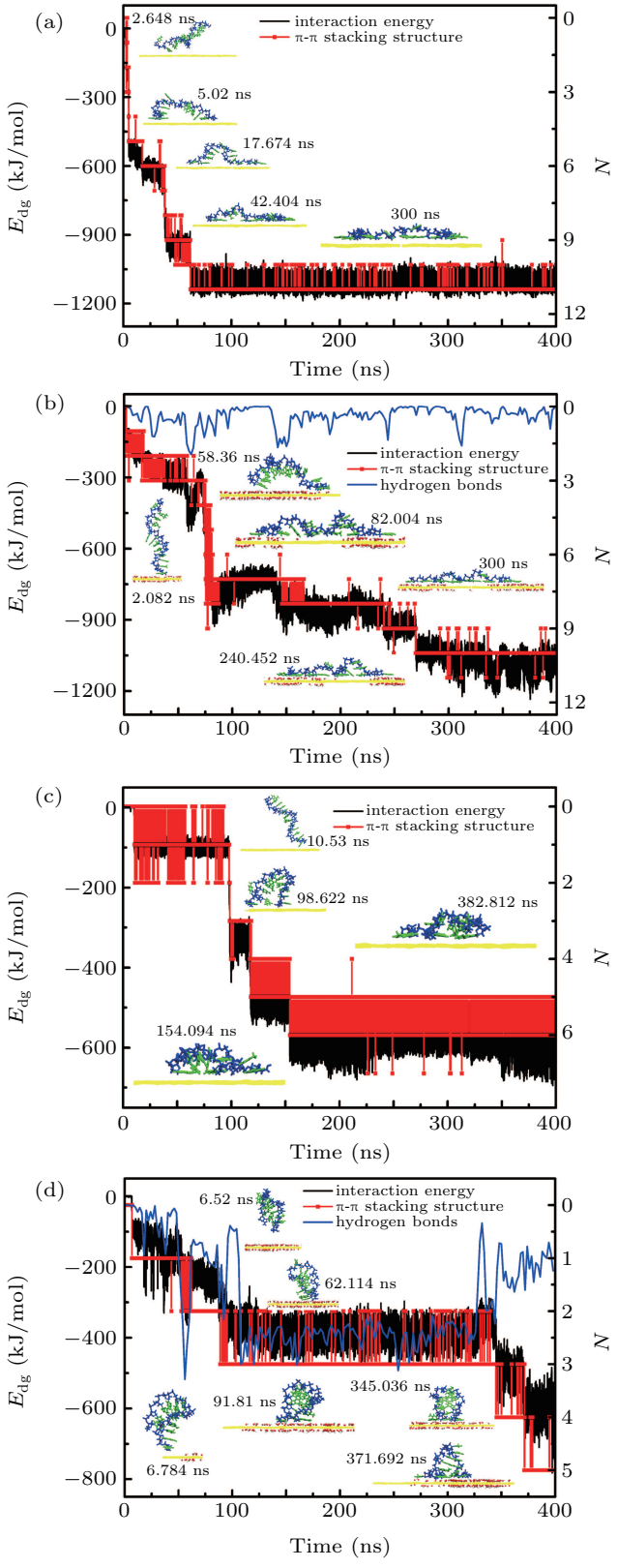


Fig. 2. Analysis of the entire dynamic process of ssDNA adsorption on PG with the adsorption configuration of stretched (a) or curved (c). Analysis of the entire dynamic process of ssDNA adsorption on GO-5% with the adsorption configuration of stretched (b) or curved (d). Black curve was E_{dg}, red curve was the number of π–π stacking between the ssDNA and the graphene-based surface, blue curve was the number of hydrogen bonds between ssDNA and GO surface.

on PG surface as the stretched configuration than the curved due to larger E_{dg} of about −1187.68 kJ/mol and greater number of π–π stacking between PG and ssDNA of 11. There was no hydrogen bond forming between PG and ssDNA molecules because of the lack of the oxidized groups on PG surface.

As for the absorption process of ssDNA molecules onto GO-5% surface, the stable adsorption time were about 269 ns and 378 ns for the stretched and curved configurations, respectively, which were much longer compared to that onto PG surface. As shown in Figs. 2(b) and 2(d), it was noted that there was a great difference of hydrogen bonds between ssDNA molecules and GO-5% surface as the stretched and curved configurations. For the stretched configuration, the number of hydrogen bonds kept around 0 with some fluctuation along whole 400 ns. This meant that ssDNA molecules mostly were adsorbed in the unoxidized region of the GO-5% surface with the stretched configuration.

Due to the atomic level smooth of the unoxidized region, ssDNA molecules could move in the unoxidized region during the dynamic adsorption process, and then occasionally contact the boundary of the oxidized region. This was the reason that the hydrogen bonds fluctuated with 0. While for the curved configuration, the number of hydrogen bonds increased first to 3, kept relatively stable, and then decreased to about 1. The ssDNA molecules were adsorbed totally or partly on the oxidized regions. During the dynamic adsorption process, ssDNA molecules were adsorbed on the GO surface with the cooperation of hydrogen binding and π–π stacking. As for GO-10%, GO-15%, GO-20% and GO-25%, the calculation results of E_{dg}, number of π–π stacking and hydrogen bonds between ssDNA and GO surfaces were shown in supporting information (Figs. S4 and S5).

3.3. Analysis of ssDNA after stable adsorption

3.3.1. Structural characteristics of ssDNA adsorbed on graphene-based surface

Based on the distinguished adsorption configurations of ssDNA molecule, we then carefully analyzed their adsorption orientation by calculating the distribution of angle α between the inter π–π stacking structures of nucleobases and graphene-based surfaces within last 20 ns. The result was shown in Fig. 3(a). There was an obvious difference between the GO-25% surface and the other graphene-based surface. For GO-25% surface, it was a broad distribution from 0° to 90°, and two peaks appeared around 15° and 45°. For PG and GO surface with oxidation degree from around 5% to 20%, α intensively distributed within 0°–10° and a single peak appeared around 10°. For PG/GO-5% nanosheet, 89.6%/80.4% of α was distributed within 0°–10°, indicating that most of the adsorbed nucleobases formed approximately parallel structure on the PG/GO-5% surface. Then, the percentage of α within 0°–10° for the GO-10% and GO-20% was about 67.0%, but 71.2% for GO-15%. As for the GO-25%, the α accounted for

38.5% at 0°–10° and 34.6% at 10°–20°. For moderate and high oxidation degrees, more adsorbed nucleobases formed approximately parallel structure on the GO-15% surface.

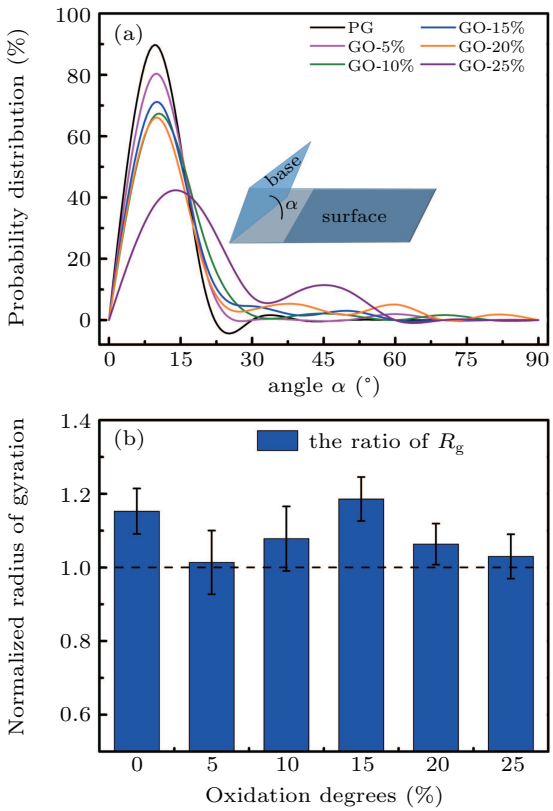


Fig. 3. (a) Distribution of angle α between the inter π-π stacking structures of nucleobases and graphene-based surfaces in last 20 ns. (b) Normalized radius of gyration for ssDNA molecules which adsorption on graphene-based surface with variable oxidation degrees.

To characterize the stretched and curved configuration of absorbed ssDNA molecules on graphene-based surface, we analyzed the radius of gyration (R_g) for the ssDNA molecules in every simulation sample and normalized according to their initial configurations. As shown in Fig. S3(b), R_g oscillated from about 1.3 nm to a stable value with a maximum of 2.0 nm and a minimum of 0.8 nm. It was shown that there were both stretched and curved configurations compared with the initial ssDNA configuration on all graphene-based surfaces. The averaged R_g for different oxidized degree GO nanosheets were shown in Fig. 3(b). The average R_g of PG approximately equaled to that of GO-15%. The R_g of GO-10% and GO-20% had the similar value, so did the GO-5% and GO-25%. This unexpected symmetry was resulted from the similar number of the curved configurations. There were only one sample of ssDNA molecule showing a curved configuration, which means ssDNA tends to be stretched on PG or GO-15%. For GO-5% and GO-25%, ssDNA showed curved configuration in three samples. For GO-10% and GO-20%, ssDNA showed curved configuration in two samples. The trend of the averaged R_g did not follow that of the oxidized degree, but similar to that of the π–π stacking and the vdW interaction, except for that on the PG. Furthermore, we also found the normalized R_g was maximum when ssDNA adsorption on GO-15% as shown in Fig. 3(b), indicating ssDNA molecules adsorbed on GO-15% had the most relax configuration.

3.3.2. In-plane movement of the absorbed ssDNA molecules on graphene-based surface

Since the absorption of ssDNA on graphene-based surface was a dynamically stable state with some fluctuation, we then analyzed the movement of ssDNA on surface by calculating its displacement within last 20 ns. The displacement of ssDNA centroid for each simulation sample and the average result were shown in Figs. 4(a) and 4(b), respectively. We noted that ssDNA molecule was more likely to move on the surface of low oxidation degree, especially on PG. As the oxidation degree of the surface increased, the adsorption of ssDNA was in more stable state, making it harder for ssDNA to move.

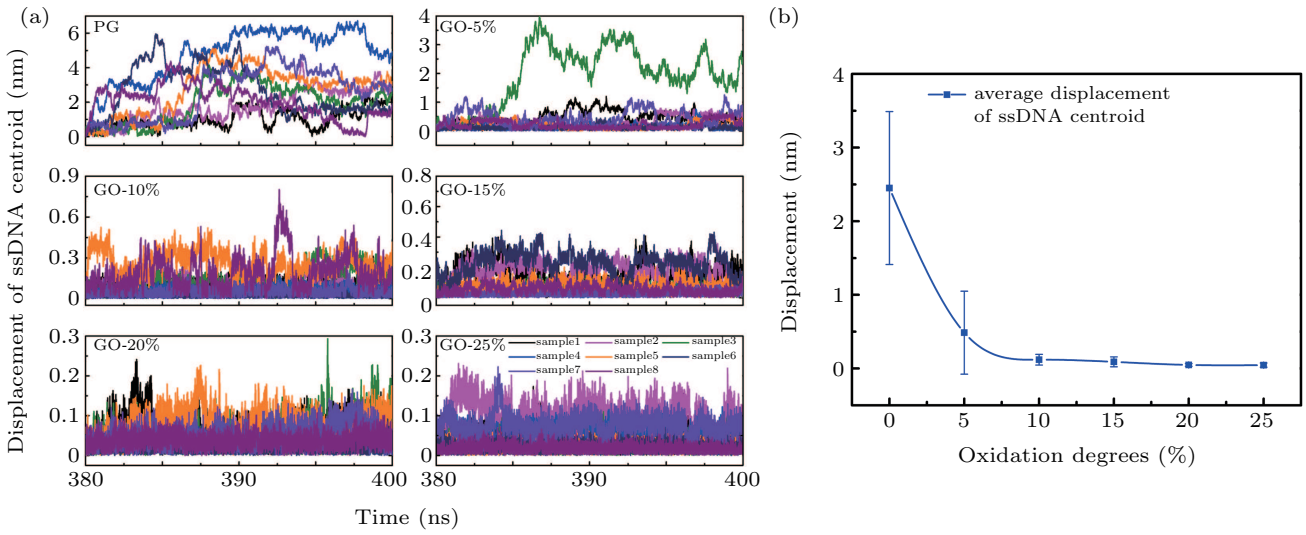


Fig. 4. (a) Displacement of ssDNA molecule on each graphene-based surface within last 20 ns. (b) Averaged displacement of the ssDNA centroid.

4. Conclusion

In this work, based on Shi–Tu model, we performed the all-atom MD simulations to investigate the ssDNA physisorption dynamics on the graphene-based surfaces with the oxidation degree ranging from 0 to 25%. By analyzing the stable configurations of the absorbed ssDNA molecules, we found that it could be absorbed in the most stable state on GO-15% according due to the total interactions between the ssDNA molecules and GO that included both vdW and electrostatic interactions. We also found that vdW interaction between them did not vary monotonously with the oxidation degree and the GO-15% held the greatest value. This result was consistent with the number of π–π stacking between ssDNA and graphene-based surface. Our analysis also showed that, the less oxidation degree on graphene-based surface relates to the greater probability for ssDNA forming the approximately parallel structure, regardless of the coexistence of both stretched and curved configurations. Our work revealed the detailed absorbed configurations of ssDNA molecules onto the graphene-based surface and provided a theoretical guidance for the applications of DNA/GO nanomaterials.

Acknowledgments

We gratefully acknowledge Prof. Guosheng Shi, Dr. Rongzheng Wan and Dr. Yongshun Song for the helpful discussions and their crucial reading of this manuscript. This work is also supported by the supercomputer Center of the Chinese Academy of Sciences, and the Shanghai Supercomputer Center of China.

References

[1] Watson J D and Crick F H 1953 *Nature* **171** 737
[2] Pray L 2008 *Nature Education* **1**
[3] Liu Z, Liu B, Ding J and Liu J 2014 *Anal. Bioanal. Chem.* **406** 6885
[4] Hu K, Lan D, Li X and Zhang S 2008 *Anal. Chem.* **80** 9124
[5] Robinson D B, Persson H H J, Zeng H, Li G, Pourmand N, Sun S and Wang S X 2005 *Langmuir* **21** 3096
[6] Song B, Cuniberti G, Sanvito S and Fang H 2012 *Appl. Phys. Lett.* **100** 063101
[7] Morales-Narváez E and Merkoçi A 2019 *Adv. Mater.* **31** 1805043
[8] Yang K, Feng L, Shi X and Liu Z 2013 *Chem. Soc. Rev.* **42** 530
[9] Tang L, Wang Y and Li J 2015 *Chem. Soc. Rev.* **44** 6954
[10] Kim J, Cote L J, Kim F, Yuan W, Shull K R and Huang J 2010 *J. Am. Chem. Soc.* **132** 8180
[11] Lu N, Wang L, Lv M, Tang Z and Fan C 2019 *Nano Res.* **12** 247
[12] Lu C, Huang Z, Liu B, Liu Y, Ying Y and Liu J 2017 *Angew. Chem. Int. Edit.* **56** 6208
[13] Liu B and Liu J 2017 *J. Am. Chem. Soc.* **139** 9471
[14] Geim A K 2009 *Science* **324** 1530
[15] Rao C, Subrahmanyam K, Ramakrishna Matte H, Maitra U, Moses K and Govindaraj A 2011 *Int. J. Mod. Phys. B* **25** 4107
[16] Nair R R, Blake P, Grigorenko A N, Novoselov K S, Booth T J, Stauber T, Peres N M and Geim A K 2008 *Science* **320** 1308
[17] Qin Zhang H Z, Xin Lu Cheng 2018 *Chin. Phys. B* **27** 27301
[18] Zheng Q, Geng Y, Wang S, Li Z and Kim J K 2010 *Carbon* **48** 4315
[19] Pumera M 2013 *Electrochem. Commun.* **36** 14
[20] Kemp K C, Seema H, Saleh M, Le N H, Mahesh K, Chandra V and Kim K S 2013 *Nanoscale* **5** 3149
[21] Lei H, Mi L, Zhou X, Chen J, Hu J, Guo S and Zhang Y 2011 *Nanoscale* **3** 3888
[22] Tu Y S, Zhao L, Sun J J, Wu Y Y, Zhou X J, Chen L, Lei X L, Fang H P and Shi G S 2020 *Chin. Phys. Lett.* **37** 066803
[23] Lei H, Mi L, Zhou X, Chen J, Hu J, Guo S and Zhang Y 2011 *Nanoscale* **3** 3888
[24] Tiwari J N, Kemp K C, Nath K, Tiwari R N, Nam H G and Kim K S 2013 *ACS Nano* **7** 9223
[25] Shankla M and Aksimentiev A 2014 *Nat. Commun.* **5** 5171
[26] Balapanuru J, Yang J X, Xiao S, Bao Q, Jahan M, Polavarapu L, Wei J, Xu Q H and Loh K P 2010 *Angew. Chem. Int. Edit.* **49** 6549
[27] Park J S, Na H K, Min D H and Kim D E 2013 *Analyst* **138** 1745
[28] Huang P J J and Liu J 2012 *Anal. Chem.* **84** 4192
[29] Varghese N, Mogera U, Govindaraj A, Das A, Maiti P K, Sood A K and Rao C 2009 *Chem. Phys. Chem.* **10** 206
[30] Manohar S, Mantz A R, Bancroft K E, Hui C Y, Jagota A and Vezenov D V 2008 *Nano Lett.* **8** 4365
[31] Jin L, Yang K, Yao K, Zhang S, Tao H, Lee S T, Liu Z and Peng R 2012 *ACS Nano* **6** 4864
[32] Patil A J, Vickery J L, Scott T B and Mann S 2009 *Adv. Mater.* **21** 3159
[33] Zhao X 2011 *J. Phys. Chem. C* **115** 6181
[34] Ma H, Xu Z, Fang H and Lei X 2020 *Phys. Chem. Chem. Phys.* **22** 11740
[35] Lei X, Ma H and Fang H 2020 *Nanoscale* **12** 6699
[36] Heerema S J and Dekker C 2016 *Nat. Nanotechn.* **11** 127
[37] Lerf A, He H, Forster M and Klinowski J 1998 *J. Phys. Chem. B* **102** 4477
[38] Gao W, Alemany L B, Ci L and Ajayan P M 2009 *Nat. Chem.* **1** 403
[39] Pacilé D, Meyer J, Rodríguez A F, Papagno M, Gomez-Navarro C, Sundaram R, Burghard M, Kern K, Carbone C and Kaiser U 2011 *Carbon* **49** 966
[40] Gómez-Navarro C, Meyer J C, Sundaram R S, Chuvilin A, Kurasch S, Burghard M, Kern K and Kaiser U 2010 *Nano Lett.* **10** 1144
[41] Erickson K, Erni R, Lee Z, Alem N, Gannett W and Zettl A 2010 *Adv. Mater.* **22** 4467
[42] Saxena S, Tyson T A and Negusse E 2010 *J. Phys. Chem. Lett.* **1** 3433
[43] Novoselov K S, Geim A K, Morozov S V, Jiang D, Zhang Y, Dubonos S V, Grigorieva I V and Firsov A A 2004 *Science* **306** 666
[44] Kronberg B, Stenius P and Igeborn G 1984 *J. Coll. Inter. Sci.* **102** 418
[45] Kim H S, Farmer B L and Yingling Y G 2017 *Adv. Mater. Inte.* **4** 1601168
[46] Yan H, Tao X, Yang Z, Li K, Yang H, Li A and Cheng R 2014 *J. Hazard. Mater.* **268** 191
[47] Tan P, Bi Q, Hu Y, Fang Z, Chen Y and Cheng J 2017 *Appl. Sur. Sci.* **423** 1141
[48] Tu Y, Lv M, Xiu P, Huynh T, Zhang M, Castelli M, Liu Z, Huang Q, Fan C and Fang H 2013 *Nat. Nanotech.* **8** 594
[49] Kim H S, Farmer B L and Yingling Y G 2017 *Adv. Mater. Inter.* **4** 1601168
[50] Yang J, Shi G, Tu Y and Fang H 2014 *Angew. Chem. Int. Edit.* **53** 10190
[51] Hess B, Kutzner C, Van Der Spoel D and Lindahl E 2008 *J. Chem. Theory Comput.* **4** 435
[52] Duan Y, Wu C, Chowdhury S, Lee M C, Xiong G, Zhang W, Yang R, Cieplak P, Luo R and Lee T 2003 *J. Comput. Chem.* **24** 1999
[53] Ponomarev S Y, Thayer K M and Beveridge D L 2004 *Proc. Nat. Acad. Sci. USA* **101** 14771
[54] Ricci C G, de Andrade A S, Mottin M and Netz P A 2010 *J. Phys. Chem. B* **114** 9882
[55] Chen J, Chen L, Wang Y and Chen S 2014 *J. Phys. D* **47** 505401
[56] Wu Y Y, Bao L, Zhang X and Tan Z J 2015 *J. Chem. Phys.* **142** 125103
[57] Xu Z, Lei X, Tu Y, Tan Z J, Song B and Fang H 2017 *Chem. Eur. J.* **23** 13100
[58] Zuo G, Zhou X, Huang Q, Fang H and Zhou R 2011 *J. Phys. Chem. C* **115** 23323
[59] Titov A V, Král P and Pearson R 2009 *ACS Nano.* **4** 229
[60] Patra N, Wang B and Král P 2009 *Nano Lett.* **9** 3766
[61] Jorgensen W L, Chandrasekhar J, Madura J D, Impey R W and Klein M L 1983 *J. Chem. Phys.* **79** 926
[62] Darden T, York D and Pedersen L 1993 *J. Chem. Phys.* **98** 10089
[63] Zeng S, Chen L, Wang Y and Chen J 2015 *J. Phys. D* **48** 275402
[64] Ranganathan S V, Halvorsen K, Myers C A, Robertson N M, Yigit M V and Chen A A 2016 *Langmuir* **32** 6028